# Supporting Information for
# Elastic deformability and luminescence of crystals of polyhalogenated platinum(II)-bipyridine complexes

Masaki Yoshida,[a,*] Yusuke Makino,[a] Toshiyuki Sasaki,[b] Shunichi Sakamoto,[b] Satoshi Takamizawa,[b] Atsushi Kobayashi,[a] and Masako Kato[a,c,*]

[a] Department of Chemistry, Faculty of Science, Hokkaido University, North-10 West-8, Kita-ku, Sapporo, Hokkaido 060-0810, Japan.

[b] Department of Materials System Science, Yokohama City University, 22-2 Seto, Kanazawa-ku, Yokohama, Kanagawa 236-0027, Japan.

[c] Department of Applied Chemistry for Environment, School of Biological and Environmental Sciences, Kwansei Gakuin University, 2-1 Gakuen, Sanda, Hyogo 669-1337, Japan.

E-mail: myoshida@sci.hokudai.ac.jp (M.Y.), katom@kwansei.ac.jp (M.K.)

**Table of Contents**

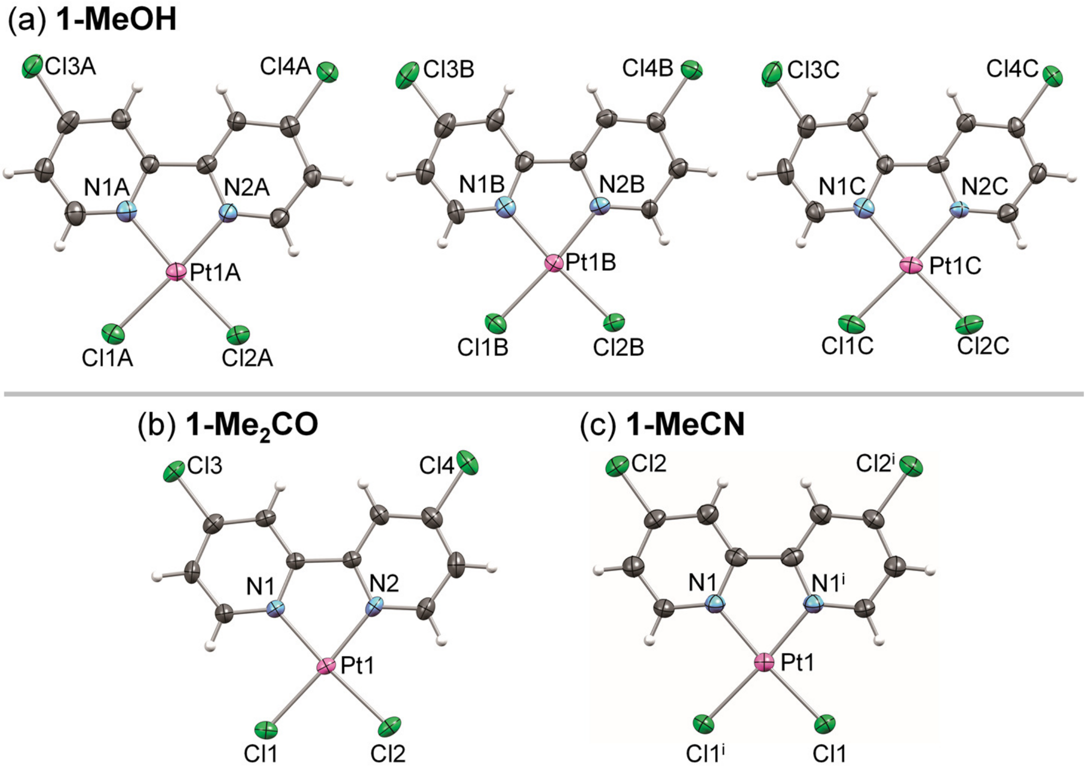

**Fig. S1** Molecular structures of (a) **1-MeOH**, (b) **1-Me$_2$CO**, and (c) **1-MeCN**. Thermal ellipsoids are displayed at the 50% probability level.

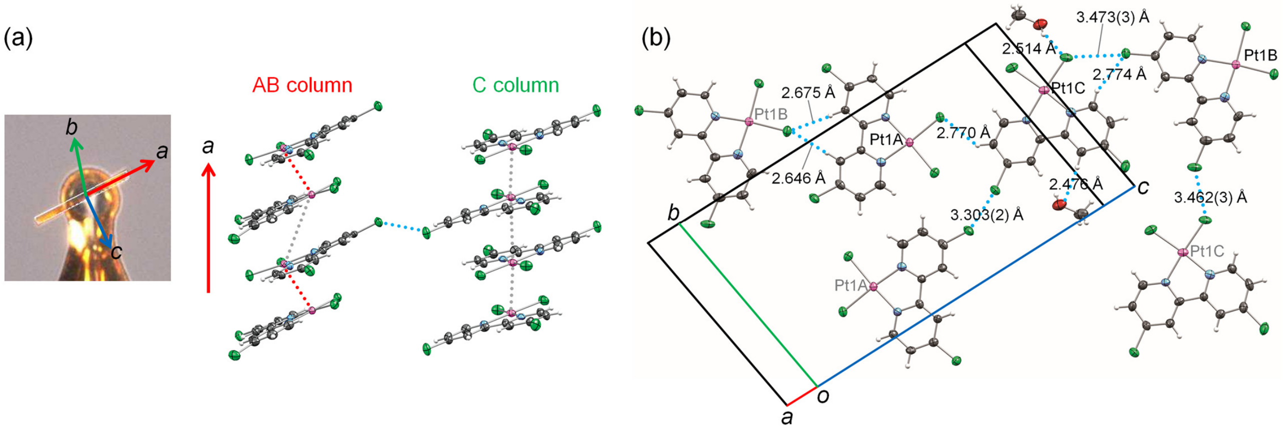

**Fig. S2** (a) The assignment of stacking direction and (b) the important intermolecular interactions of **1-MeOH**. Thermal ellipsoids are displayed at the 50% probability level.

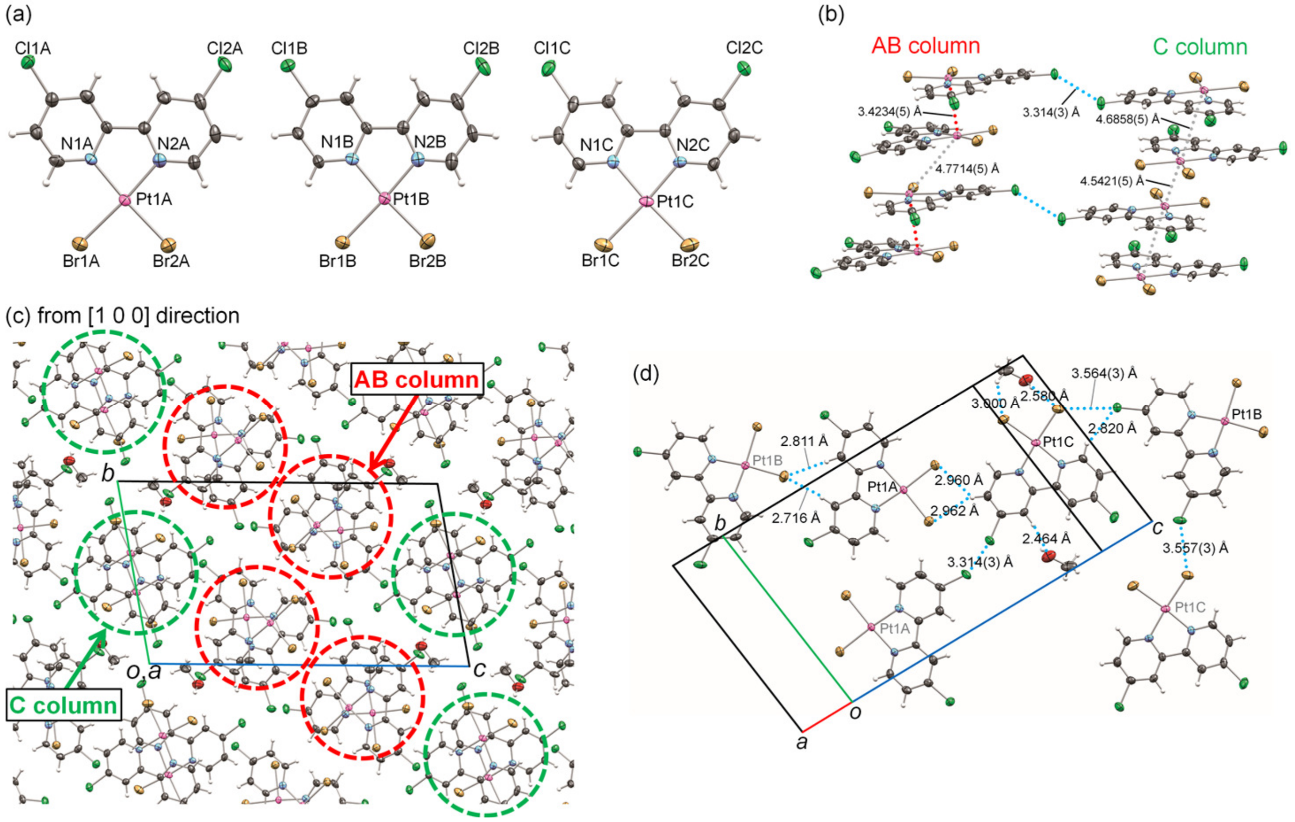

**Fig. S3** (a) Molecular and (b) stacking structures of **2-MeOH**, (c) packing structures of **2-MeOH** viewed from the [1 0 0] direction, and (d) the important interatomic interactions. Thermal ellipsoids are displayed at the 50% probability level.

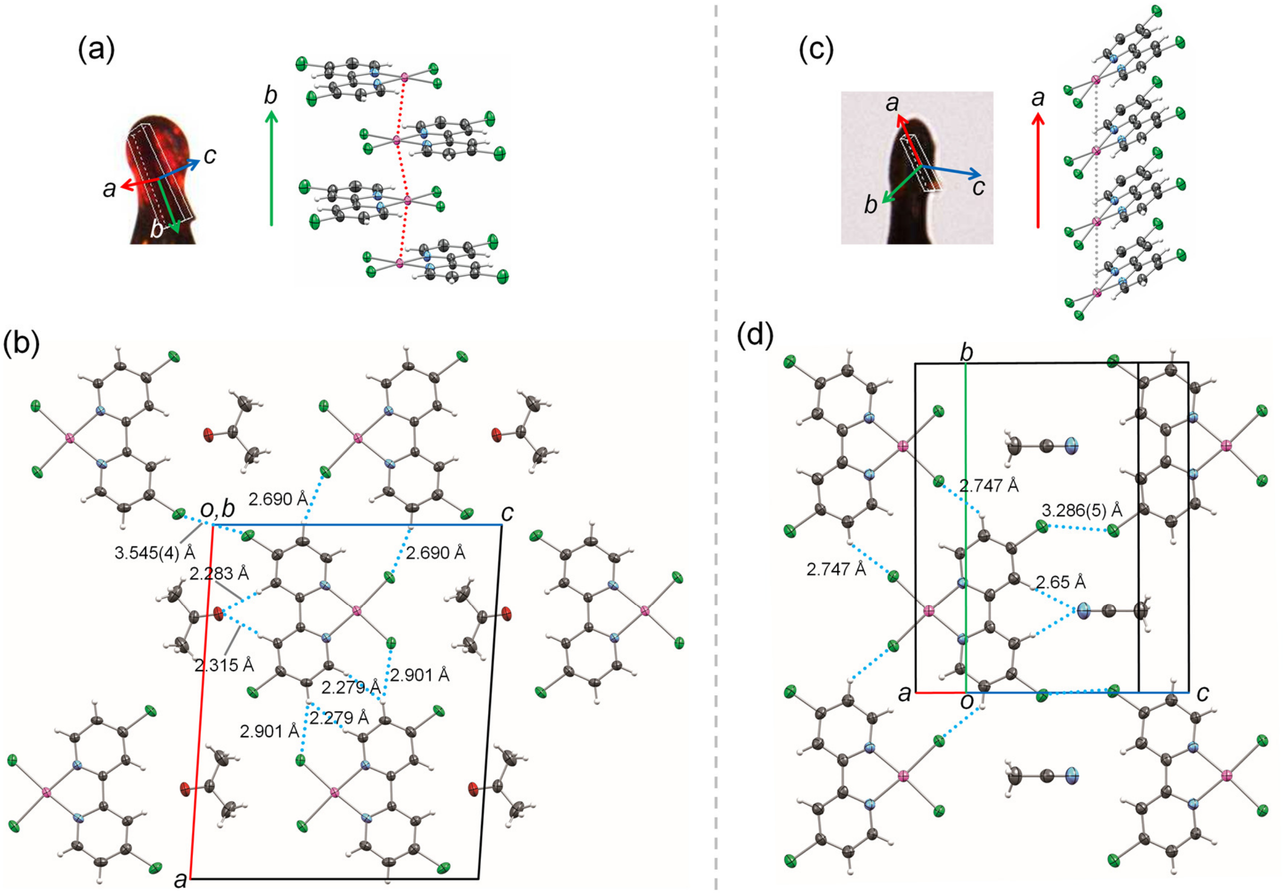

**Fig. S4** (a,c) The assignment of stacking direction and (b,d) the important intermolecular interactions of (a,b) **1-Me$_2$CO** and (b,c) **1-MeCN**. Thermal ellipsoids are displayed at the 50% probability level.

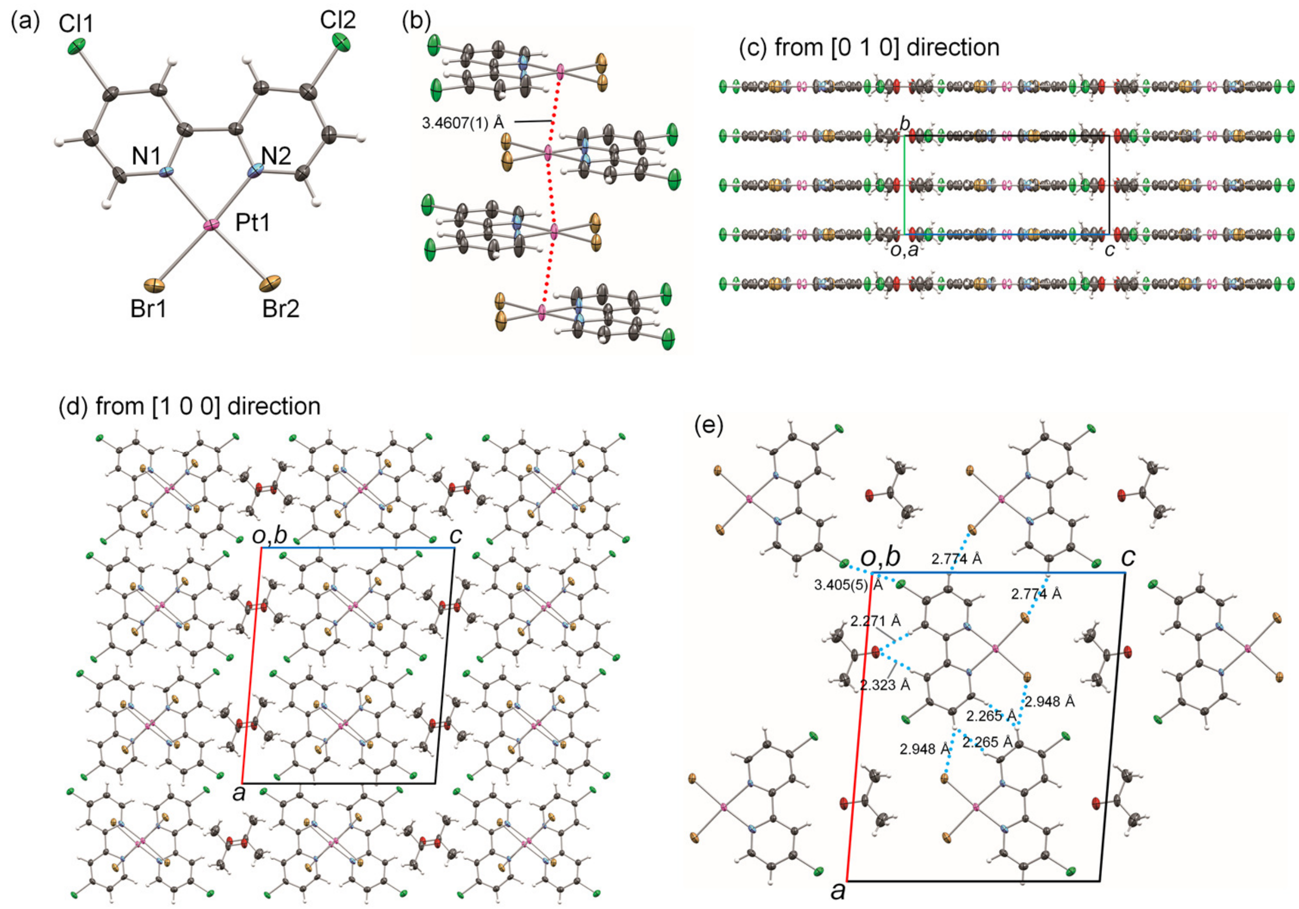

**Fig. S5** (a) Molecular and (b) stacking structures of **2-Me$_2$CO**, (c,d) packing structures of **2-Me$_2$CO** viewed from (c) the [0 1 0] and (d) the [1 0 0] directions, and (e) the important interatomic interactions. Thermal ellipsoids are displayed at the 50% probability level.

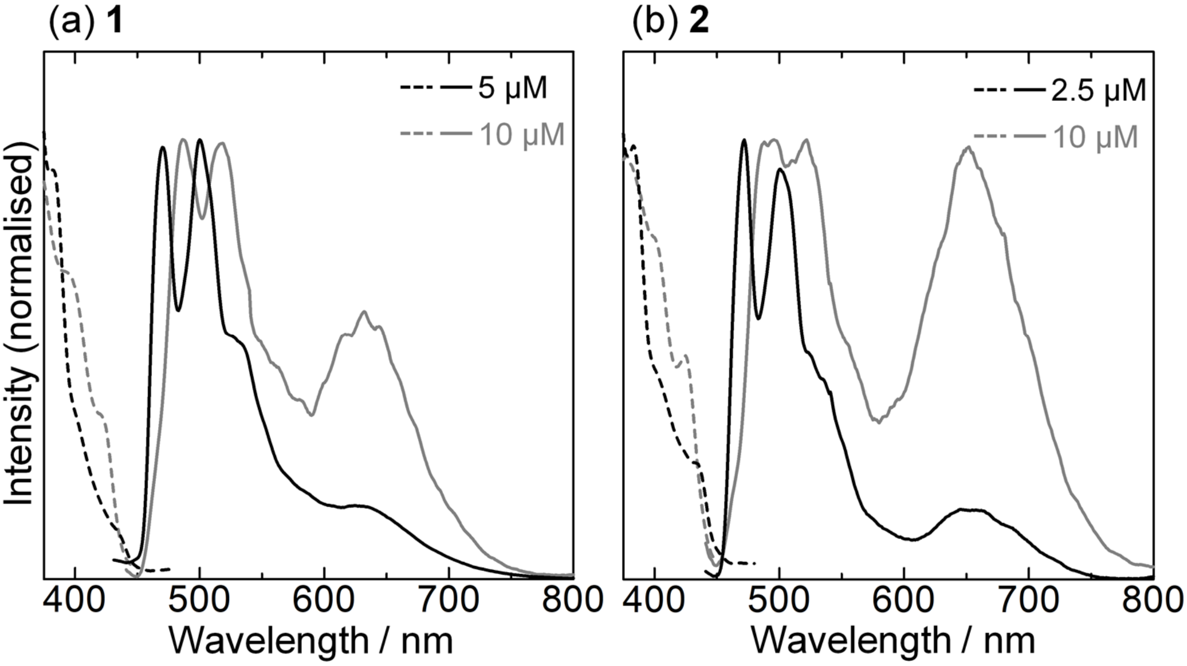

**Fig. S6** Emission (solid lines, $\lambda_{ex}$ = 350 nm) and excitation (dashed lines) spectra of (a) **1** and (b) **2** in the MeOH/EtOH [1:1 (v/v)] glass at 77 K. The detection wavelengths for the excitation spectra were 500 nm (**1**, 5 μM), 486 nm (**1**, 10 μM), 501 nm (**2**, 2.5 μM), and 488 nm (**2**, 10 μM). These complexes exhibited vibrationally structured emission bands around 470 nm in the MeOH/EtOH [1:1 (v/v)] glass, indicating that the discrete monomer-derived emissions of these complexes are not originated from $^3$MC but from $^3\pi\pi^*$ excited states. On the other hand, the broad structureless emission bands at around 640 nm increased with increasing the concentration of the complexes, which can be attributed to the $^3$MMLCT emission from the assembled state.

Three-point bending test experiments were carried out by using a universal testing machine at room temperature. Single crystal was put on two-point support and then force was applied on crystal by a metal-blade jig in the strain range of 0.01 (Fig. S7(a)). The face of the crystal was pushed downward (press) by the jig at a displacement rate of 2 μm sec$^{-1}$. After some extent of bending the force was released to recover crystal to its original shape. In these experiments one crystal was analyzed by varying the distance between two-point support/basement.

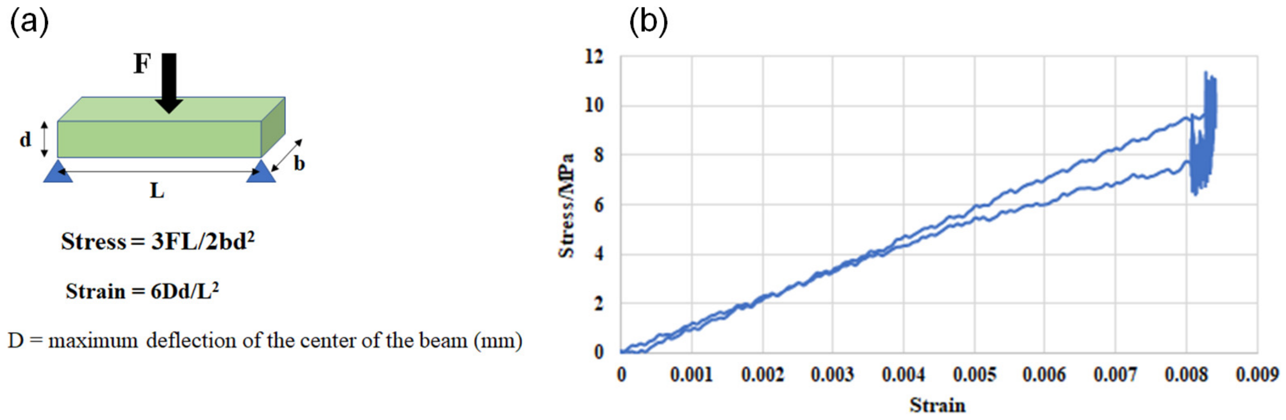

**Fig. S7** (a) Experimental setup. The stress and strain applied to the sample was calculated from the equations above using crystal dimensions. (b) The stress-strain curve of a single crystal of **1-MeCN** (dimension L = 2.5 mm, b = 0.0.0871 mm, and d = 0.039 mm), showing the elastic bending-restoration cycle (The disarrangement of stress at the reflecting point was caused by a slight slippage of the jig at the contact point on the curved specimen). The estimated elastic modulus (1.2 GPa) is almost consistent with that estimated from the vibrating reed method (Table S3).

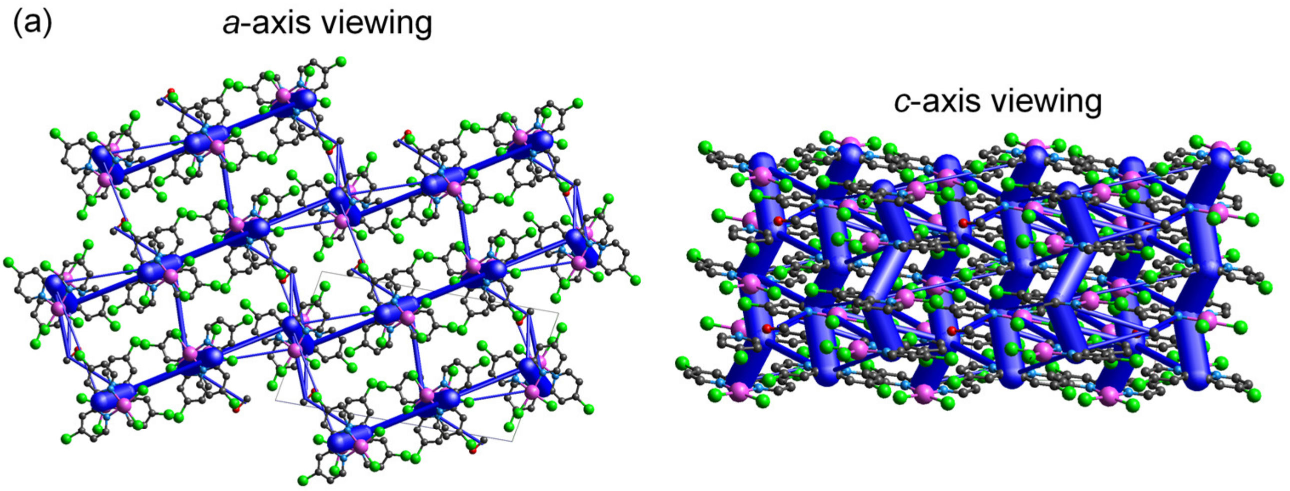

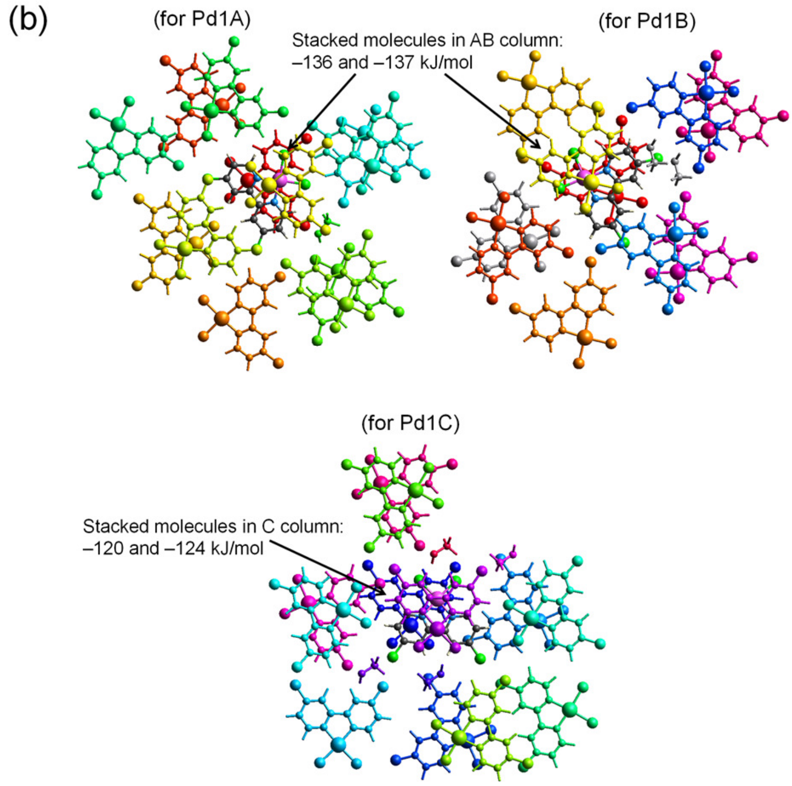

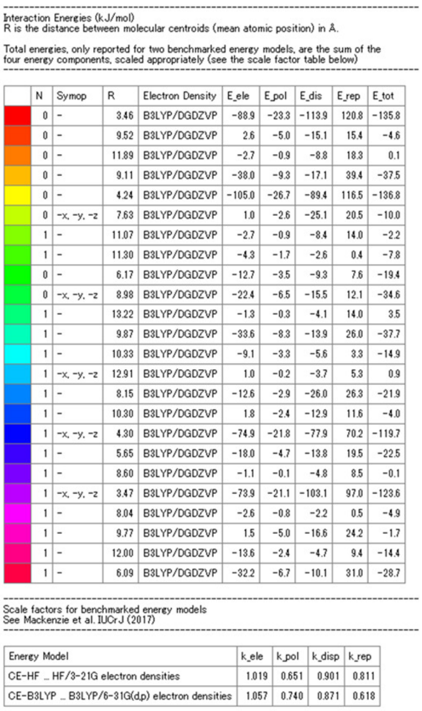
Interaction Energies (kJ/mol)
R is the distance between molecular centroids (mean atomic position) in Å.

Total energies, only reported for two benchmarked energy models, are the sum of the four energy components, scaled appropriately (see the scale factor table below)

|  | N | Symop | R | Electron Density | E_ele | E_pol | E_dis | E_rep | E_tot |
|---|---|---|---|---|---|---|---|---|---|
| 🟥 | 0 | - | 3.46 | B3LYP/DGDZVP | −88.9 | −23.3 | −113.9 | 120.8 | −135.8 |
| 🟥 | 0 | - | 9.52 | B3LYP/DGDZVP | 2.6 | −5.0 | −15.1 | 15.4 | −4.6 |
| 🟧 | 0 | - | 11.89 | B3LYP/DGDZVP | −2.7 | −0.9 | −8.8 | 18.3 | 0.1 |
| 🟧 | 0 | - | 9.11 | B3LYP/DGDZVP | −38.0 | −9.3 | −17.1 | 39.4 | −37.5 |
| 🟨 | 0 | - | 4.24 | B3LYP/DGDZVP | −105.0 | −26.7 | −89.4 | 116.5 | −136.8 |
| 🟩 | 0 | −x, −y, −z | 7.63 | B3LYP/DGDZVP | 1.0 | −2.6 | −25.1 | 20.5 | −10.0 |
| 🟩 | 1 | - | 11.07 | B3LYP/DGDZVP | −2.7 | −0.9 | −8.4 | 14.0 | −2.2 |
| 🟩 | 1 | - | 11.30 | B3LYP/DGDZVP | −4.3 | −1.7 | −2.6 | 0.4 | −7.8 |
| 🟩 | 0 | - | 6.17 | B3LYP/DGDZVP | −12.7 | −3.5 | −9.3 | 7.6 | −19.4 |
| 🟩 | 0 | −x, −y, −z | 8.98 | B3LYP/DGDZVP | −22.4 | −6.5 | −15.5 | 12.1 | −34.6 |
| 🟩 | 1 | - | 13.22 | B3LYP/DGDZVP | −1.3 | −0.3 | −4.1 | 14.0 | 3.5 |
| 🟩 | 1 | - | 9.87 | B3LYP/DGDZVP | −33.6 | −8.3 | −13.9 | 26.0 | −37.7 |
| 🟦 | 1 | - | 10.33 | B3LYP/DGDZVP | −9.1 | −3.3 | −5.6 | 3.3 | −14.9 |
| 🟦 | 1 | −x, −y, −z | 12.91 | B3LYP/DGDZVP | 1.0 | −0.2 | −3.7 | 5.3 | 0.9 |
| 🟦 | 1 | - | 8.15 | B3LYP/DGDZVP | −12.6 | −2.9 | −26.0 | 26.3 | −21.9 |
| 🟦 | 1 | - | 10.30 | B3LYP/DGDZVP | 1.8 | −2.4 | −12.9 | 11.6 | −4.0 |
| 🟦 | 1 | −x, −y, −z | 4.30 | B3LYP/DGDZVP | −74.9 | −21.8 | −77.9 | 70.2 | −119.7 |
| 🟪 | 1 | - | 5.65 | B3LYP/DGDZVP | −18.0 | −4.7 | −13.8 | 19.5 | −22.5 |
| 🟪 | 1 | - | 8.60 | B3LYP/DGDZVP | −1.1 | −0.1 | −4.8 | 8.5 | −0.1 |
| 🟪 | 1 | −x, −y, −z | 3.47 | B3LYP/DGDZVP | −73.9 | −21.1 | −103.1 | 97.0 | −123.6 |
| 🟪 | 1 | - | 8.04 | B3LYP/DGDZVP | −2.6 | −0.8 | −2.2 | 0.5 | −4.9 |
| 🟪 | 1 | - | 9.77 | B3LYP/DGDZVP | 1.5 | −5.0 | −16.6 | 24.2 | −1.7 |
| 🟥 | 1 | - | 12.00 | B3LYP/DGDZVP | −13.6 | −2.4 | −4.7 | 9.4 | −14.4 |
| 🟥 | 1 | - | 6.09 | B3LYP/DGDZVP | −32.2 | −6.7 | −10.1 | 31.0 | −28.7 |

Scale factors for benchmarked energy models
See Mackenzie et al. IUCrJ (2017)

| Energy Model | k_ele | k_pol | k_disp | k_rep |
|---|---|---|---|---|
| CE-HF … HF/3-21G electron densities | 1.019 | 0.651 | 0.901 | 0.811 |
| CE-B3LYP … B3LYP/6-31G(d,p) electron densities | 1.057 | 0.740 | 0.871 | 0.618 |

**Fig. S8** (a) Energy frameworks of **1’-MeOH** in total interaction strengths viewed along the *a*- and the *c*-axes. (b) The interaction energies of various molecular dimers estimated using the CE-B3LYP method.

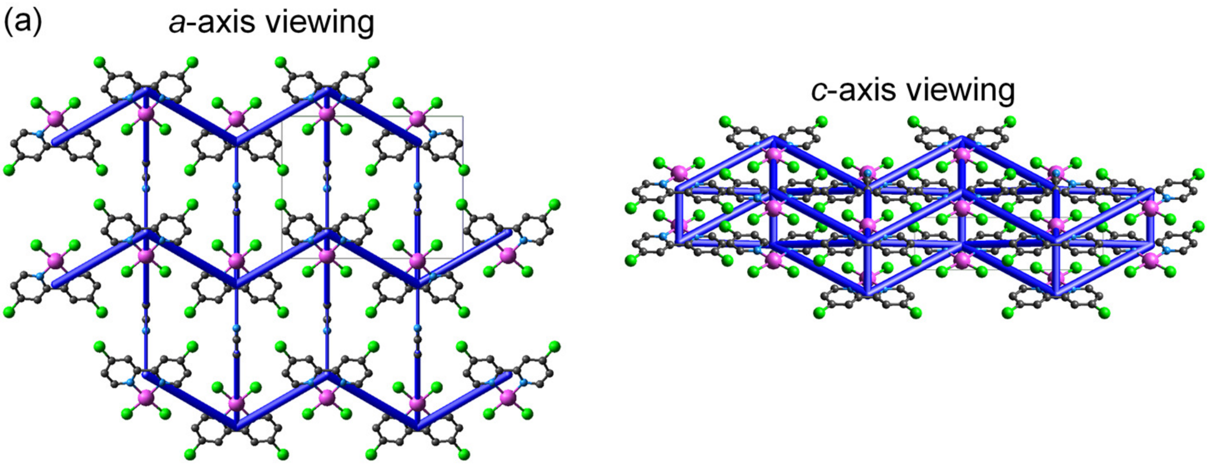

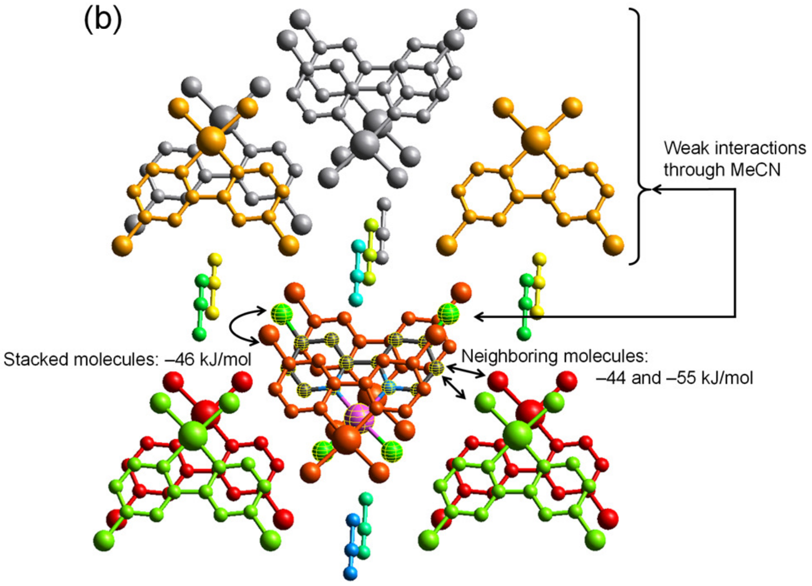

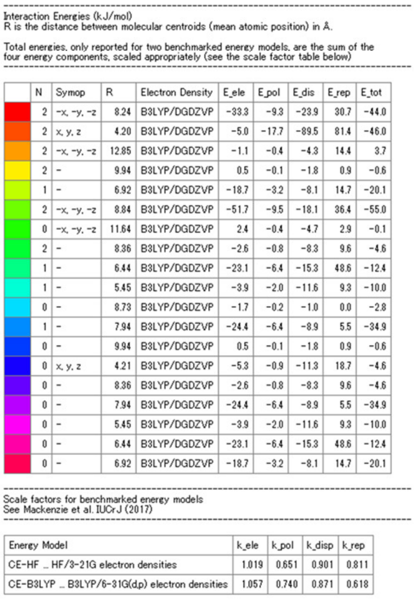

Interaction Energies (kJ/mol)
R is the distance between molecular centroids (mean atomic position) in Å.

Total energies, only reported for two benchmarked energy models, are the sum of the four energy components, scaled appropriately (see the scale factor table below)

| | N | Symop | R | Electron Density | E_ele | E_pol | E_dis | E_rep | E_tot |
|---|---|---|---|---|---|---|---|---|---|
| 🟥 | 2 | −x, −y, −z | 8.24 | B3LYP/DGDZVP | −33.3 | −9.3 | −23.9 | 30.7 | −44.0 |
| 🟧 | 2 | x, y, z | 4.20 | B3LYP/DGDZVP | −5.0 | −17.7 | −89.5 | 81.4 | −46.0 |
| 🟧 | 2 | −x, −y, −z | 12.85 | B3LYP/DGDZVP | −1.1 | −0.4 | −4.3 | 14.4 | 3.7 |
| 🟨 | 2 | − | 9.94 | B3LYP/DGDZVP | 0.5 | −0.1 | −1.8 | 0.9 | −0.6 |
| 🟩 | 1 | − | 6.92 | B3LYP/DGDZVP | −18.7 | −3.2 | −8.1 | 14.7 | −20.1 |
| 🟩 | 2 | −x, −y, −z | 8.84 | B3LYP/DGDZVP | −51.7 | −9.5 | −18.1 | 36.4 | −55.0 |
| 🟩 | 0 | −x, −y, −z | 11.64 | B3LYP/DGDZVP | 2.4 | −0.4 | −4.7 | 2.9 | −0.1 |
| 🟩 | 2 | − | 8.36 | B3LYP/DGDZVP | −2.6 | −0.8 | −8.3 | 9.6 | −4.6 |
| 🟩 | 1 | − | 6.44 | B3LYP/DGDZVP | −23.1 | −6.4 | −15.3 | 48.6 | −12.4 |
| 🟦 | 1 | − | 5.45 | B3LYP/DGDZVP | −3.9 | −2.0 | −11.6 | 9.3 | −10.0 |
| 🟦 | 0 | − | 8.73 | B3LYP/DGDZVP | −1.7 | −0.2 | −1.0 | 0.0 | −2.8 |
| 🟦 | 1 | − | 7.94 | B3LYP/DGDZVP | −24.4 | −6.4 | −8.9 | 5.5 | −34.9 |
| 🟦 | 0 | − | 9.94 | B3LYP/DGDZVP | 0.5 | −0.1 | −1.8 | 0.9 | −0.6 |
| 🟦 | 0 | x, y, z | 4.21 | B3LYP/DGDZVP | −5.3 | −0.9 | −11.3 | 18.7 | −4.6 |
| 🟪 | 0 | − | 8.36 | B3LYP/DGDZVP | −2.6 | −0.8 | −8.3 | 9.6 | −4.6 |
| 🟪 | 0 | − | 7.94 | B3LYP/DGDZVP | −24.4 | −6.4 | −8.9 | 5.5 | −34.9 |
| 🟪 | 0 | − | 5.45 | B3LYP/DGDZVP | −3.9 | −2.0 | −11.6 | 9.3 | −10.0 |
| 🟪 | 0 | − | 6.44 | B3LYP/DGDZVP | −23.1 | −6.4 | −15.3 | 48.6 | −12.4 |
| 🟥 | 0 | − | 6.92 | B3LYP/DGDZVP | −18.7 | −3.2 | −8.1 | 14.7 | −20.1 |

Scale factors for benchmarked energy models
See Mackenzie et al. IUCrJ (2017)

| Energy Model | k_ele | k_pol | k_disp | k_rep |
|---|---|---|---|---|
| CE-HF ... HF/3-21G electron densities | 1.019 | 0.651 | 0.901 | 0.811 |
| CE-B3LYP ... B3LYP/6-31G(d,p) electron densities | 1.057 | 0.740 | 0.871 | 0.618 |

**Fig. S9** (a) Energy frameworks of **1’-MeCN** in total interaction strengths viewed along the *a*- and the *c*-axes. (b) The interaction energies of various molecular dimers estimated using the CE-B3LYP method.

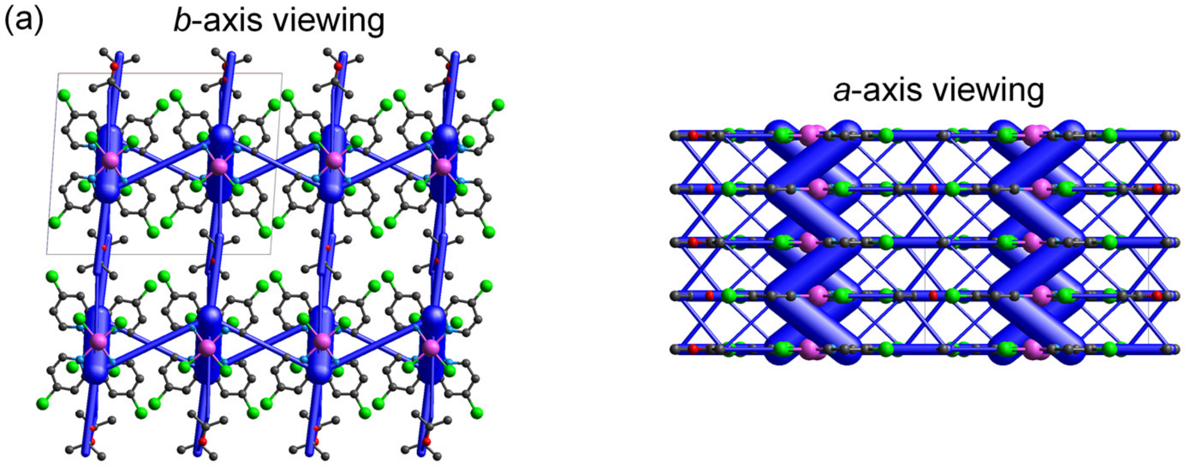

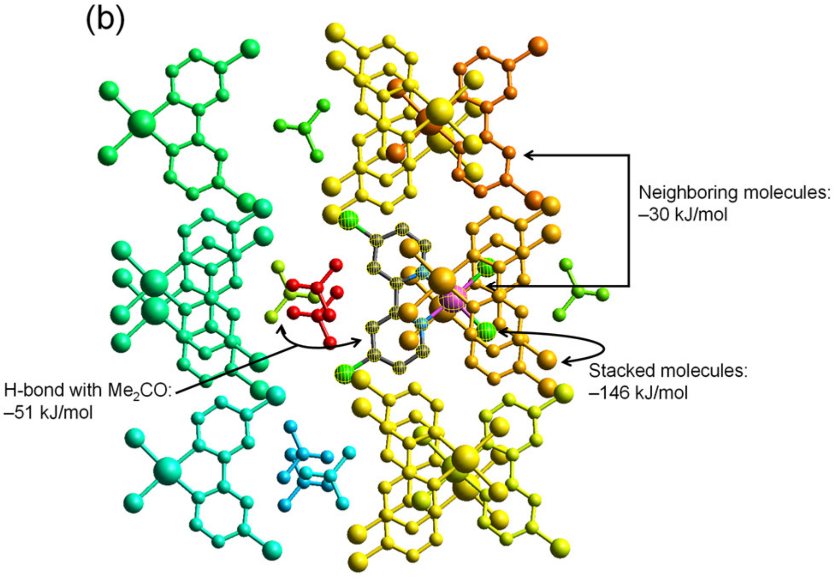

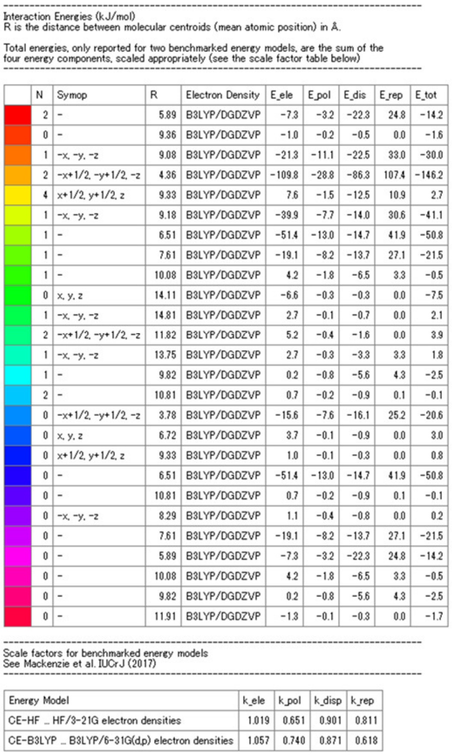

Interaction Energies (kJ/mol)
R is the distance between molecular centroids (mean atomic position) in Å.

Total energies, only reported for two benchmarked energy models, are the sum of the four energy components, scaled appropriately (see the scale factor table below)

| | N | Symop | R | Electron Density | E_ele | E_pol | E_dis | E_rep | E_tot |
|---|---|---|---|---|---|---|---|---|---|
| 🟥 | 2 | - | 5.89 | B3LYP/DGDZVP | −7.3 | −3.2 | −22.3 | 24.8 | −14.2 |
| 🟥 | 0 | - | 9.36 | B3LYP/DGDZVP | −1.0 | −0.2 | −0.5 | 0.0 | −1.6 |
| 🟧 | 1 | −x, −y, −z | 9.08 | B3LYP/DGDZVP | −21.3 | −11.1 | −22.5 | 33.0 | −30.0 |
| 🟧 | 2 | −x+1/2, −y+1/2, −z | 4.36 | B3LYP/DGDZVP | −109.8 | −28.8 | −86.3 | 107.4 | −146.2 |
| 🟨 | 4 | x+1/2, y+1/2, z | 9.33 | B3LYP/DGDZVP | 7.6 | −1.5 | −12.5 | 10.9 | 2.7 |
| 🟨 | 1 | −x, −y, −z | 9.18 | B3LYP/DGDZVP | −39.9 | −7.7 | −14.0 | 30.6 | −41.1 |
| 🟩 | 1 | - | 6.51 | B3LYP/DGDZVP | −51.4 | −13.0 | −14.7 | 41.9 | −50.8 |
| 🟩 | 1 | - | 7.61 | B3LYP/DGDZVP | −19.1 | −8.2 | −13.7 | 27.1 | −21.5 |
| 🟩 | 1 | - | 10.08 | B3LYP/DGDZVP | 4.2 | −1.8 | −6.5 | 3.3 | −0.5 |
| 🟩 | 0 | x, y, z | 14.11 | B3LYP/DGDZVP | −6.6 | −0.3 | −0.3 | 0.0 | −7.5 |
| 🟩 | 1 | −x, −y, −z | 14.81 | B3LYP/DGDZVP | 2.7 | −0.1 | −0.7 | 0.0 | 2.1 |
| 🟩 | 2 | −x+1/2, −y+1/2, −z | 11.82 | B3LYP/DGDZVP | 5.2 | −0.4 | −1.6 | 0.0 | 3.9 |
| 🟩 | 1 | −x, −y, −z | 13.75 | B3LYP/DGDZVP | 2.7 | −0.3 | −3.3 | 3.3 | 1.8 |
| 🟦 | 1 | - | 9.82 | B3LYP/DGDZVP | 0.2 | −0.8 | −5.6 | 4.3 | −2.5 |
| 🟦 | 2 | - | 10.81 | B3LYP/DGDZVP | 0.7 | −0.2 | −0.9 | 0.1 | −0.1 |
| 🟦 | 0 | −x+1/2, −y+1/2, −z | 3.78 | B3LYP/DGDZVP | −15.6 | −7.6 | −16.1 | 25.2 | −20.6 |
| 🟦 | 0 | x, y, z | 6.72 | B3LYP/DGDZVP | 3.7 | −0.1 | −0.9 | 0.0 | 3.0 |
| 🟦 | 0 | x+1/2, y+1/2, z | 9.33 | B3LYP/DGDZVP | 1.0 | −0.1 | −0.3 | 0.0 | 0.8 |
| 🟦 | 0 | - | 6.51 | B3LYP/DGDZVP | −51.4 | −13.0 | −14.7 | 41.9 | −50.8 |
| 🟪 | 0 | - | 10.81 | B3LYP/DGDZVP | 0.7 | −0.2 | −0.9 | 0.1 | −0.1 |
| 🟪 | 0 | −x, −y, −z | 8.29 | B3LYP/DGDZVP | 1.1 | −0.4 | −0.8 | 0.0 | 0.2 |
| 🟪 | 0 | - | 7.61 | B3LYP/DGDZVP | −19.1 | −8.2 | −13.7 | 27.1 | −21.5 |
| 🟪 | 0 | - | 5.89 | B3LYP/DGDZVP | −7.3 | −3.2 | −22.3 | 24.8 | −14.2 |
| 🟥 | 0 | - | 10.08 | B3LYP/DGDZVP | 4.2 | −1.8 | −6.5 | 3.3 | −0.5 |
| 🟥 | 0 | - | 9.82 | B3LYP/DGDZVP | 0.2 | −0.8 | −5.6 | 4.3 | −2.5 |
| 🟥 | 0 | - | 11.91 | B3LYP/DGDZVP | −1.3 | −0.1 | −0.3 | 0.0 | −1.7 |

Scale factors for benchmarked energy models
See Mackenzie et al. IUCrJ (2017)

| Energy Model | k_ele | k_pol | k_disp | k_rep |
|---|---|---|---|---|
| CE-HF ... HF/3-21G electron densities | 1.019 | 0.651 | 0.901 | 0.811 |
| CE-B3LYP ... B3LYP/6-31G(d,p) electron densities | 1.057 | 0.740 | 0.871 | 0.618 |

**Fig. S10** (a) Energy frameworks of **1’-Me$_2$CO** in total interaction strengths viewed along the *b*- and the *a*-axes. (b) The interaction energies of various molecular dimers estimated using the CE-B3LYP method.

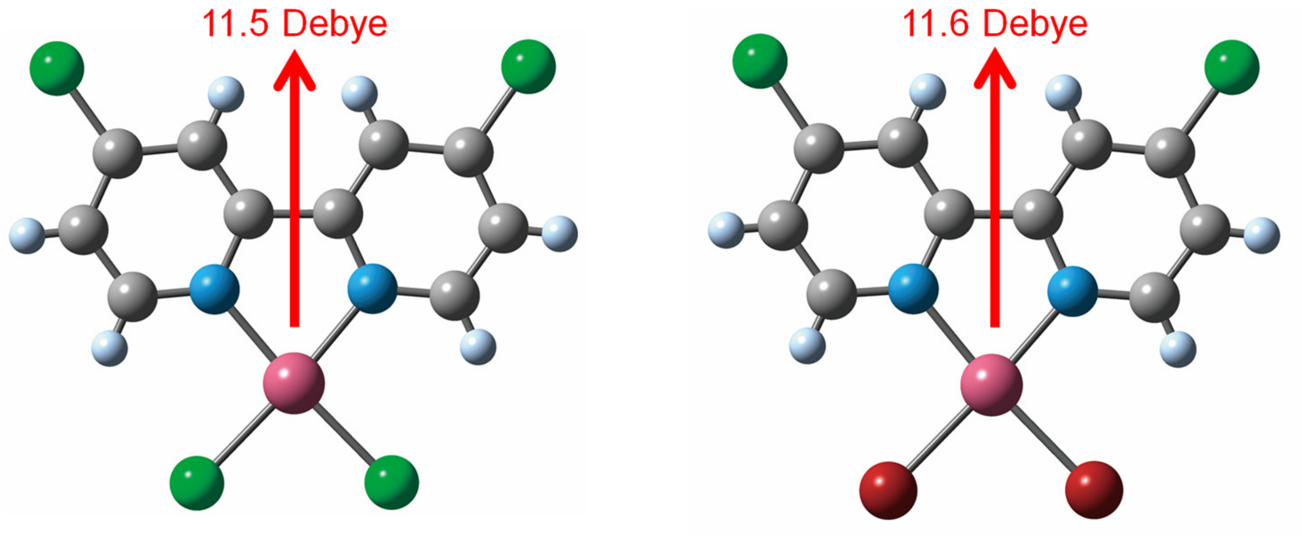

**Fig. S11** Calculated dipole moments of **1** (left) and **2** (right). Molecular structures were taken from experimental crystal geometries of **1-MeCN** and **2-Me$_2$CO** without optimisation.

**Table S1** Selected interatomic distances (Å) and angles (deg) of **1-MeOH**, **1-Me$_2$CO**, and **1-MeCN**.

| | **1-MeOH** (A) | **1-MeOH** (B) | **1-MeOH** (C) | **1-Me$_2$CO** | **1-MeCN** |
|---|---|---|---|---|---|
| Distances / Å | | | | | |
| Pt1-N1 | 2.020(5) | 2.018(6) | 2.035(6) | 2.006(5) | 2.023(9) |
| Pt1-N2 | 2.025(6) | 2.001(5) | 2.014(5) | 2.006(5) | – |
| Pt1-Cl1 | 2.295(2) | 2.292(2) | 2.299(2) | 2.304(2) | 2.292(3) |
| Pt1-Cl2 | 2.301(2) | 2.295(2) | 2.290(2) | 2.301(2) | – |
| Pt1-Pt1 | 3.3708(4), 4.7698(5)<br>(for column AB) | | 4.5127(4),<br>4.6598(4)<br>(for column C) | 3.40719(7) | 4.2050(1) |
| Angles / deg | | | | | |
| N1-Pt1-N2 | 81.0(2) | 80.0(2) | 80.6(2) | 80.6(2) | 80.1(5)$^a$ |
| N1-Pt1-Cl1 | 95.1(2) | 94.9(2) | 95.2(2) | 95.3(2) | 95.5(3)$^b$ |
| N1-Pt1-Cl2 | 174.0(2) | 175.7(2) | 175.4(2) | 175.4(2) | 175.6(3)$^c$ |
| N2-Pt1-Cl1 | 175.6(2) | 174.6(2) | 175.8(2) | 175.9(1) | – |
| N2-Pt1-Cl2 | 94.3(2) | 95.8(2) | 94.8(2) | 94.8(2) | – |
| Cl1-Pt1-Cl2 | 89.71(6) | 89.38(6) | 89.36(7) | 89.33(6) | 88.8(1)$^d$ |

$^a$ N1-Pt1-N1$^i$. $^b$ N1$^i$-Pt1-Cl1. $^c$ N1-Pt1-Cl1$^i$. $^d$ Cl1-Pt1-Cl1$^i$.

**Table S2** Selected interatomic distances (Å) and angles (deg) of **2-MeOH** and **2-Me$_2$CO**.

| | **2-MeOH** (A) | **2-MeOH** (B) | **2-MeOH** (C) | **2-Me$_2$CO** |
|---|---|---|---|---|
| Distances / Å | | | | |
| Pt1-N1 | 2.042(7) | 2.022(7) | 2.033(7) | 2.018(7) |
| Pt1-N2 | 2.022(7) | 2.023(7) | 2.023(7) | 2.029(8) |
| Pt1-Br1 | 2.416(1) | 2.414(1) | 2.413(1) | 2.4197(9) |
| Pt1-Br2 | 2.412(1) | 2.395(1) | 2.415(1) | 2.409(1) |
| Pt1-Pt1 | 3.4234(5), 4.7714(5)<br>(for column AB) | | 4.5421(5),<br>4.6858(5)<br>(for column C) | 3.4607(1) |
| Angles / deg | | | | |
| N1-Pt1-N2 | 81.1(3) | 80.2(3) | 80.6(3) | 79.7(3) |
| N1-Pt1-Br1 | 94.6(2) | 96.4(2) | 95.4(2) | 96.2(2) |
| N1-Pt1-Br2 | 175.8(2) | 174.5(2) | 175.4(2) | 175.6(2) |
| N2-Pt1-Br1 | 174.2(2) | 176.4(2) | 176.0(2) | 176.0(2) |
| N2-Pt1-Br2 | 94.9(2) | 94.7(2) | 94.9(2) | 95.8(2) |
| Br1-Pt1-Br2 | 89.47(4) | 88.74(4) | 89.05(4) | 88.20(4) |

The elastic modulus $E$ (Pa) was calculated on a formula (1):[S1]

$$E = \left(\frac{2 f_n \pi l^2}{\lambda_n^2}\right)^2 \frac{\rho A}{I} \tag{1}$$

where $f$ is resonance frequency (Hz), $l$ is length of a vibrating part of a crystal specimen (m), $\lambda_n$ are 1.875 (n=1) and 4.694 (n=2), $\rho$ is density (kg m$^{-3}$), $A$ is cross-sectional area (m$^2$), and $I$ is sectional moment of inertia (m$^4$). Sectional moment of inertia for a specimen with a rectangular section is calculated on the following equation (2):

$$I = \frac{bh^3}{12} \tag{2}$$

where $b$ and $h$ are length of a rectangular section (m) perpendicular and parallel to vibrating direction, respectively.

**Table S3** Elastic modulus (Young's modulus) of **1-MeCN** and related parameters. The estimated elastic modulus is almost consistent with that estimated from the stress-strain curve (1.2 GPa; Fig. S7).

| Vibrating direction | Crystal size / m$^3$ | $\rho$ / kg m$^{-3}$ | $f$ / Hz | $E$ / GPa |
|---|---|---|---|---|
| $S$ (shorter axis) | $(879 \times 10^{-6}) \times (37.2 \times 10^{-6}) \times (21.8 \times 10^{-6})$ | 2.339 | 1181 | 0.62 |
| $H$ (middle axis) | | | 2613 | 1.1 |

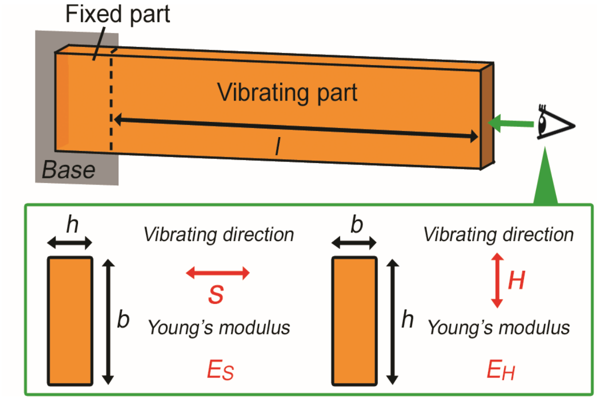

**Table S4.** Crystal parameters and refinement data.

| | **1-MeOH** | **1-Me$_2$CO** | **1-MeCN** | **2-MeOH** | **2-Me$_2$CO** |
|---|---|---|---|---|---|
| CCDC No. | 2073739 | 2073740 | 2073741 | 2073742 | 2073743 |
| Formula | $C_{10.33}H_{7.33}Cl_4N_2O_{0.33}Pt$ | $C_{13}H_{12}Cl_4N_2OPt$ | $C_{12}H_9Cl_4N_3Pt$ | $C_{10.33}H_{7.33}Br_2Cl_2N_2O_{0.33}Pt$ | $C_{13}H_{12}Br_2Cl_2N_2OPt$ |
| Formula weight | 501.74 | 549.14 | 532.11 | 590.66 | 638.06 |
| Crystal system | Triclinic | Monoclinic | Monoclinic | Triclinic | Monoclinic |
| Space group | $P\bar{1}$ (#2) | $C2/m$ (#12) | $P2_1/m$ (#11) | $P\bar{1}$ (#2) | $C2/m$ (#12) |
| $a$ (Å) | 7.3163(2) | 17.3962(4) | 4.2050(1) | 7.4532(1) | 17.5085(2) |
| $b$ (Å) | 12.5322(4) | 6.7242(1) | 15.1349(4) | 12.7323(2) | 6.8605(1) |
| $c$ (Å) | 22.0934(3) | 14.1075(3) | 11.8849(4) | 22.1827(3) | 14.2988(2) |
| $\alpha$ (deg) | 99.217(2) | 90 | 90 | 99.629(1) | 90 |
| $\beta$ (deg) | 97.693(2) | 93.761(2) | 92.547(3) | 98.186(1) | 94.738(1) |
| $\gamma$ (deg) | 94.038(2) | 90 | 90 | 94.794(1) | 90 |
| $V$ (Å$^3$) | 1972.82(9) | 1646.68(6) | 755.63(4) | 2041.78(5) | 1711.66(4) |
| $Z$ | 6 | 4 | 2 | 6 | 4 |
| $D_{calc}$ (g cm$^{-1}$) | 2.534 | 2.215 | 2.339 | 2.882 | 2.476 |
| $T$ (K) | 150 | 150 | 150 | 150 | 150 |
| Reflns collected | 24125 | 5205 | 4364 | 24010 | 5802 |
| Unique reflns | 8060 | 1828 | 1589 | 8301 | 1906 |
| GOF on $F^2$ | 1.065 | 1.125 | 1.093 | 1.097 | 1.075 |
| $R_{int}$ | 0.0420 | 0.0339 | 0.0559 | 0.0460 | 0.0393 |
| $R_1$ ($I > 2\sigma(I)$)[a] | 0.0337 | 0.0295 | 0.0605 | 0.0395 | 0.0393 |
| w$R_2$[b] | 0.1050 | 0.0822 | 0.1723 | 0.1086 | 0.1093 |

[a] $R_1 = \Sigma||F_o|-|F_c|| / \Sigma|F_o|$. [b] $wR_2 = [\Sigma w(F_o^2 - F_c^2)/ \Sigma w(F_o)^2]^{1/2}$, $w = [\sigma_c^2(F_o^2) + (xP)^2 + yP]^{-1}$, $P = (F_o^2 - 2F_c^2)/3$.

## References.

[S1] (a) M. Horio and S. Onogi, *J. Appl. Phys.*, 1951, **22**, 977–981; (b) D. R. Bland and E. H. Lee, *J. Appl. Phys.*, 1955, **26**, 1497–1503; (c) K. Hashimoto, M. Sakane, M. Ohnami and T. Yoshida, *J. Soc. Mater. Sci., Jpn.*, 1995, **44**, 1456–1463; (d) T. Sasaki, S. Sakamoto, K. Nishizawa and S. Takamizawa, *Cryst. Growth Des.*, 2020, **20**, 3913–3917.